Neural stem cells secreting bispecific T cell engager to induce selective antiglioma activity

Katarzyna C. Pituch[a,1], Markella Zannikou[a,1], Liliana Ilut[a], Ting Xiao[a], Michael Chastkofsky[a], Madina Sukhanova[b], Nicola Bertolino[c], Daniele Procissi[c], Christina Amidei[a], Craig M. Horbinski[a,b], Karen S. Aboody[d], C. David James[a], Maciej S. Lesniak[a], and Irina V. Balyasnikova[a,2]

[a]Department of Neurological Surgery, Feinberg School of Medicine, Northwestern University, Chicago, IL 60611; [b]Department of Pathology, Feinberg School of Medicine, Northwestern University, Chicago, IL 60611; [c]Department of Radiology, Feinberg School of Medicine, Northwestern University, Chicago, IL 60611; and [d]Division of Neurosurgery, Department of Neurosciences, Beckman Research Institute of the City of Hope, Duarte, CA 91010

Edited by Carl June, Raymond and Ruth Perelman School of Medicine at the University of Pennsylvania, Philadelphia, PA, and approved January 19, 2021 (received for review July 29, 2020)

Glioblastoma (GBM) is the most lethal primary brain tumor in adults. No treatment provides durable relief for the vast majority of GBM patients. In this study, we've tested a bispecific antibody comprised of single-chain variable fragments (scFvs) against T cell CD3ε and GBM cell interleukin 13 receptor alpha 2 (IL13Rα2). We demonstrate that this bispecific T cell engager (BiTE) ($BiTE^{LLON}$) engages peripheral and tumor-infiltrating lymphocytes harvested from patients' tumors and, in so doing, exerts anti-GBM activity ex vivo. The interaction of $BiTE^{LLON}$ with T cells and IL13Rα2-expressing GBM cells stimulates T cell proliferation and the production of proinflammatory cytokines interferon γ (IFNγ) and tumor necrosis factor α (TNFα). We have modified neural stem cells (NSCs) to produce and secrete the $BiTE^{LLON}$ (NSC^{LLON}). When injected intracranially in mice with a brain tumor, NSC^{LLON} show tropism for tumor, secrete $BiTE^{LLON}$, and remain viable for over 7 d. When injected directly into the tumor, NSC^{LLON} provide a significant survival benefit to mice bearing various IL13Rα2$^+$ GBMs. Our results support further investigation and development of this therapeutic for clinical translation.

bispecific T cell engagers | delivery | GBM | neural stem cells | immunotherapy

Routine treatment of newly diagnosed glioblastoma (GBM) consists of surgical resection, chemotherapy, and radiation, which results in a median GBM patient survival of less than 2 y, with just 5% of patients surviving beyond 5 y (1). The blood–brain barrier (BBB) limits therapeutic access to the tumor (2). An immunosuppressive microenvironment and molecular heterogeneity of GBM present a unique set of challenges for developing effective therapies for this type of brain tumor (3–10).

The development of treatments for lessening the immunosuppressive effects of GBM represents an active area of preclinical and clinical neuro-oncology research. Many, if not all, approaches being tested involve increasing T cell cytotoxic antitumor activity (11–17). Large numbers of functional cytotoxic tumor-infiltrating lymphocytes (TILs) correlate with improved progression-free survival for GBM patients (18–21). However, the immunosuppressive milieu of GBM impairs T cell cytolytic function, altering the effectiveness of T cell-based therapies for treating GBM (22–26). Numerous lymphocyte-directed treatments are being investigated, including the use of bispecific T cell engagers (BiTEs) (17, 27, 28). BiTEs can be produced and used without patient-specific BiTE individualization and can, therefore, be considered "off-the-shelf" therapeutics (29–32). The use of BiTEs targeting tumor-associated antigens (TAAs) has been approved by the Food and Drug Administration (FDA) in treating liquid malignancies, and BiTE-associated treatments are currently being evaluated in multiple clinical studies for solid tumors (e.g., NCT03792841, NCT04117958, and NCT03319940) (33–36).

BiTEs consist of two single-chain variable fragments (scFvs) connected by a flexible linker (37). One of the scFvs is directed to a TAA and the other to CD3 epsilon (ε) that is expressed on T cells (38). BiTEs engage TILs and cancer cells in a major histocompatibility complex (MHC)-independent manner and are, therefore, unaffected by MHC down-regulation that occurs in GBM cells (37–40). The specificity of BiTE's tumor antigen-directed scFv is imperative to harness the full therapeutic potential of the recombinant molecule (41). BiTE anticancer activity requires BiTE binding with malignant and immune cells simultaneously; single-arm binding to a tumor antigen or CD3ε is therapeutically ineffective (42, 43).

The short half-life of BiTEs in plasma necessitates a frequent or continuous infusion into patient circulation to maintain therapeutic levels of BiTE (43–45). Several approaches have been proposed and tested to compensate for the rate of BiTE biologic life in treating peripheral cancers (45–47). These include the recombinant protein's sustained production by subcutaneous injection of mesenchymal stem cells (MSCs) seeded into a synthetic extracellular matrix scaffold, liver translation of BiTE messenger RNA (mRNA), and peritumoral delivery of MSCs

Significance

Glioblastoma (GBM) is the most aggressive and lethal brain tumor in adults. The GBM microenvironment is highly immunosuppressive, rendering T cells incapable of recognizing and eliminating malignant cells. We developed bispecific T cell engagers (BiTEs) that successfully engage patients' T cells to attack and kill GBM expressing interleukin 13 receptor alpha 2 (IL13Rα2). Neural stem cells (NSCs) engineered to secrete BiTE migrate readily within the brain tissue to established tumors and produce BiTE protein within the malignant tissue. Treatment of animals bearing IL13Rα2-expressing patient-derived GBM xenografts with therapeutic NSCs resulted in significant survival benefits in mice. These results show an exciting potential of NSCs as a delivery platform for BiTE therapy to improve outcomes for GBM patients.

Author contributions: K.C.P., M.Z., and I.V.B. designed research; K.C.P., M.Z., L.I., M.C., M.S., N.B., D.P., C.A., and I.V.B. performed research; K.S.A. contributed new reagents/analytic tools; K.C.P., M.Z., T.X., M.C., M.S., N.B., D.P., C.M.H., and I.V.B. analyzed data; and K.C.P., M.Z., M.S., D.P., K.S.A., C.D.J., M.S.L., and I.V.B. wrote the paper.

Competing interest statement: I.V.B. and M.S.L. have a patent for the use of ScFv47 for IL13Rα2-targeted cancer therapies. K.S.A. holds a patent covering the use of neural stem cells for cancer therapy.

This article is a PNAS Direct Submission.

[1]K.C.P. and M.Z. contributed equally to this work.

[2]To whom correspondence may be addressed. Email: irinabal@northwestern.edu.

This article contains supporting information online at https://www.pnas.org/lookup/suppl/doi:10.1073/pnas.2015800118/-/DCSupplemental.

Published February 24, 2021.

secreting BiTEs. A recent study also explored the use of modified immune cell delivery of BiTE to GBM (48), and the reduction of tumor burden in treated animals has been observed. It remains to be determined if these bicistronic antiglioma treatments share chimeric antigen receptor (CAR) T cells' fate, which includes a low penetrance and short survival of CARs within the brain (27, 49, 50); both are limiting factors for sustained and efficient delivery of BiTEs by CAR T cells.

Neural stem cells (NSCs) have inherent advantages as a cellular carrier of antineoplastic agents to the site of GBM since they are native to the brain. NSCs have demonstrated tropism to brain tumors in several preclinical models. These cells can withstand a harsh oxygen-deprived environment of GBM. Here, we investigated NSCs as producers of BiTEs targeting the tumor-associated antigen interleukin 13 receptor alpha 2 (IL13Rα2) and their antitumor activity using in vitro and in vivo models of GBM. In vitro, BiTEs show significant antitumor activity when used in cocultures that include T cells harvested from patients' blood and tumor tissue. In vivo, NSCs modified for BiTE synthesis migrate to a tumor in animal subjects' brains while functioning as intra- and peritumoral BiTE producers. The following are details of the results from our experiments in characterizing NSCs that produce IL13Rα2-directed BiTEs. We interpret these findings as support for additional safety and efficacy analysis for their potential clinical translation in treating GBM patients.

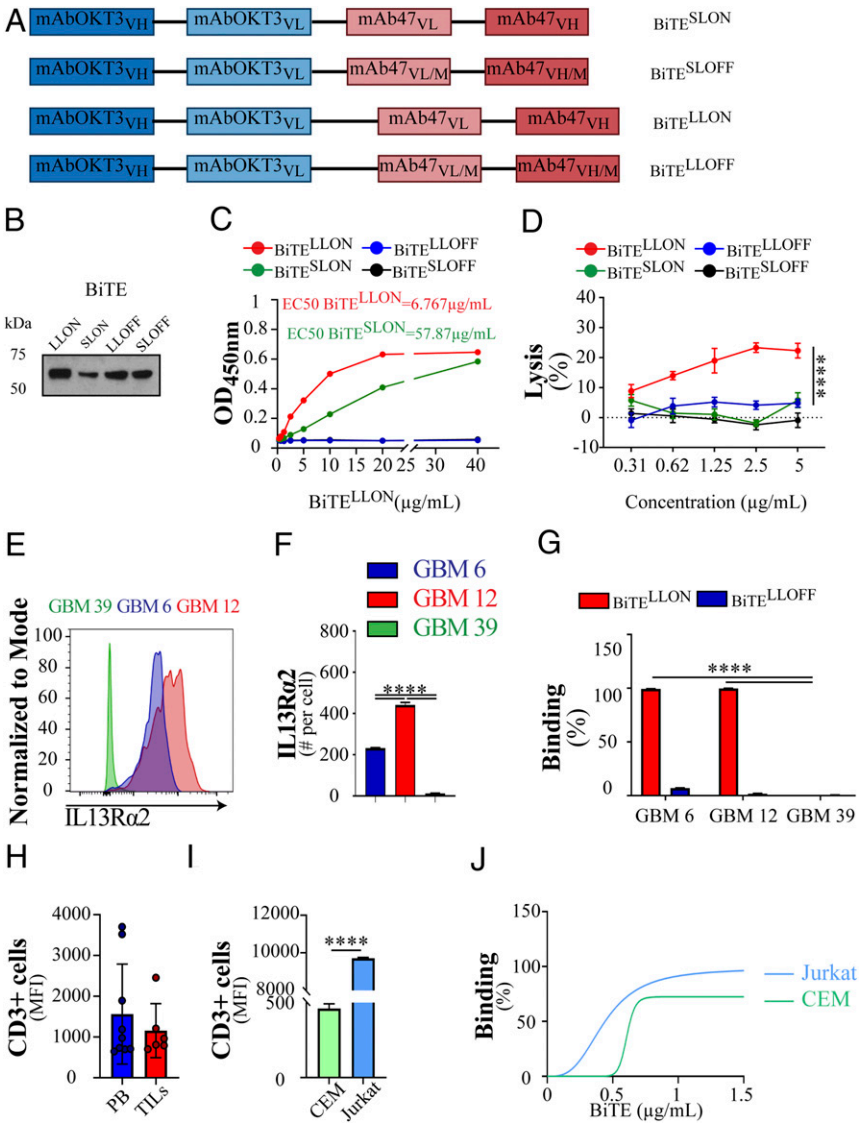

Fig. 1. Design of BiTE targeting IL13Rα2-expressing gliomas. (*A*) BiTEs consist of the scFv fragments of mAbOKT3 against the CD3ε and scFv of mAb47 against IL13Rα2 connected by either short or long linkers named as $BiTE^{SLON}$ and $BiTE^{LLON}$, respectively. The CDR3 of the light chain (VL/M) of the mA47 was replaced with a sequence of the nonspecific MOPC21 antibody to generate $BiTE^{LLOFF}$ and $BiTE^{SLOFF}$ to controls with abridged binding to IL13Rα2. (*B*) Western blotting showed a specific single band after affinity purification and detection with anti-His antibodies at ∼55 kDa. (*C*) Increasing concentration of BiTE molecules bound to human IL13Rα2 immobilized on ELISA plates (1 μg/mL) and detected using anti-His tag antibodies. EC_{50} of $BiTE^{LLON}$ is 6.767 μg/mL, and EC_{50} of $BiTE^{SLON}$ is 57.87 μg/mL. (*D*) $BiTE^{LLON}$ but not $BiTE^{LLOFF}$ engaged CDε-expressing cells from glioma patients in the killing of IL13Rα2-expressing glioma cells (target-to-effector [T:E] ratio 1:20, two-way ANOVA, $n = 3$–4, $^{****}P < 0.0001$). (*E*) Example of flow cytometry chromatogram for IL13Rα2-negative GBM39 cell line and IL13Rα2-positive cell lines, GBM6, and GBM12. (*F*) Expression of IL13Rα2 at the cell surface in GBM6, GBM12, and GBM39 cell lines (one-way ANOVA, $n = 3$, $^{****}P < 0.0001$). (*G*) Binding of $BiTE^{LLON}$ and $BiTE^{LLOFF}$ to GBM cell lines (one-way ANOVA, $n \geq 3$, $^{****}P < 0.0001$). (*H*) Expression of CD3ε on the surface of GBM patients' PB lymphocytes and TILs ($n \geq 6$). (*I*) CD3ε expression on the cell surface of CCRF-CEM, a T lymphoblastoid cell line (28), and Jurkat, a T lymphoblast cell line. (*J*) Binding of $BiTE^{LLON}$ to CEM and Jurkat cell lines ($n = 3$). OD_{450nm}, optical density at 450 nm. MFI, median fluorescent intensity.

Results

Development of Tumor-Targeting BiTEs. BiTE-targeting IL13Rα2 was generated using the scFv of mAb47 against the IL13Rα2 that has been previously described by our group and scFv of the mAb OKT3 directed toward the invariable ε chain of CD 3 (CDε) (49, 51–54). ScFvs were connected using a flexible glycine/serine linker in the following orientation: $mAbOKT3_{VH}$-$mAbOKT3_{VL}$-$mAb47_{VL}$-$mAb47_{VH}$ (Fig. 1*A*). Short (SL, 5 amino acids) and long (LL, 23 amino acids) linkers were used to construct $BiTE^{SLON}$ and $BiTE^{LLON}$. $BiTE^{SLOFF}$ and $BiTE^{LLOFF}$ control molecules were generated by replacing the complementary determinant region 3 of the mAb47 light chain with the sequence of the mAb MOPC-21, which prevents IL13Rα2 binding (Fig. 1*A*) (38). A polyhistidine (6His) tag was added at the C terminus of BiTE constructs for BiTE purification and detection. All acronyms for BiTE molecules are listed in *SI Appendix*, Table S1. Lentiviral vectors (pLVX-IRES-ZsGreen1) encoding complementary DNA (cDNA) for each BiTE were constructed, and corresponding lentiviral particles were used to transduce HEK293T cells for the production of BiTE proteins. Recombinant BiTE proteins were purified from culture supernatants using HisPure resin. Purified BiTE integrity was verified by Western blotting using anti-His antibodies (Fig. 1*B*).

Characterization of BiTE Binding and Function. Binding of purified BiTEs to IL13Rα2 and CD3ε epitopes was examined using an enzyme-linked immunosorbent assay (ELISA) and cell-binding assays. $BiTE^{LLON}$ showed 8.5× higher affinity binding to immobilized IL13Rα2 than $BiTE^{SLON}$ (effective concentration, 50% [EC_{50}] values of 6.767 μg/mL and 57.87 μg/mL, respectively) (Fig. 1*C*). Control BiTEs did not bind to IL13Rα2 (Fig. 1*C*).

A majority of gliomas express IL13Rα2, with GBM expressing it at the highest levels (*SI Appendix*, Fig. S1*A*) (55, 56). The ability of BiTEs to engage donor T cells in antiglioma activity was determined using cocultures of IL13Rα2-expressing GBM cells (*SI Appendix*, Fig. S1 *B* and *C*) with BiTEs and T cells. $BiTE^{LLON}$ successfully engages T cells, as indicated by BiTE concentration-dependent cytotoxicity, with a maximal effect observed at 2.5 μg/mL (Fig. 1*D* and *SI Appendix*, Fig. S1*D*). $BiTE^{SLON}$ did not induce T cell antitumor activity (Fig. 1*D*).

Patient-derived xenograft cell lines GBM6, GBM12, and GBM39 express different levels of IL13Rα2 (Fig. 1 *E* and *F*). $BiTE^{LLON}$ binds to GBM6, and GBM12 cells, but not to GBM39 in which IL13Rα2 is either absent or expressed at a level beneath that required for flow cytometry detection. At a concentration of 2 μg/mL, $BiTE^{LLON}$ saturates IL13Rα2 in GBM6 and -12 (Fig. 1*G*) and occupies 50% of available receptor in U251 cells (*SI Appendix*, Fig. S1*E*).

Flow cytometry analysis of GBM patient T cell CD3ε expression revealed substantial interpatient variability in peripheral blood (PB) and TIL (20) populations. CD3ε-associated fluorescence intensity ranged from 649 to 3,058 and from 706 to 1,753 for PB and TILs, respectively (Fig. 1*H*). We used human lymphocyte Jurkat and CEM cell lines to further test BiTE interaction with CD3 (Fig. 1*I* and *SI Appendix*, Fig. S1 *F* and *G*) and observed saturation binding as BiTE concentrations approached 1.5 μg/mL (Fig. 1*J*). BiTE CD3ε binding was also apparent when using IL13Rα2 binding defective $BiTE^{LLOFF}$ (*SI Appendix*, Fig. S1*H*).

To examine BiTE-induced T cell antitumor activity in vitro, we used the chromium 51 (^{51}Cr) release assay. $BiTE^{LLON}$ engaged T cell killing of IL13Rα2-expressing GBM6 and GBM12 glioma cells in a target-to-effector (T:E) ratio-dependent fashion (Fig. 2 *A* and *B*). GBM39 cells, negative for IL13Rα2 expression, were not killed by the T cells, at any tested T:E ratio, in the presence of $BiTE^{LLON}$ and $BiTE^{LLOFF}$ (Fig. 2*C*). Similar killing activity was observed with T cells harvested from the blood of a patient with another type of brain tumor, colloidal meningioma, in coculture with IL13Rα2-positive GBMs in the presence of $BiTE^{LLON}$, but not IL13Rα2-negative cells or $BiTE^{LLOFF}$ (*SI Appendix*, Fig. S2 *A–C*). At day 3 of coculturing, the majority of IL13Rα2-expressing GBM cells were killed by T cells in the presence of $BiTE^{LLON}$, but not in $BiTE^{LLOFF}$ (Fig. 2*D*). GBM cell killing was associated with proliferation and activation of T cells, as exemplified by the expression of CD69 and CD25 T cell markers. There was no proliferation or expression of activation molecules for T cells cocultured with $BiTE^{LLOFF}$, or for T cells cultured with $BiTE^{LLON}$, as well as $BiTE^{LLOFF}$ in the absence of IL13Rα2-expressing GBM cells (Fig. 2 *E–G* and *SI Appendix*, Fig. S2 *D–F*). T cell proliferation and activation were associated with significant increases in T cell secretion of IL2, interferon γ (IFNγ), and tumor necrosis factor α (TNFα) (Fig. 2 *H–J* and *SI Appendix*, Fig. G-I).

BiTE Engages GBM Patients' Lymphocytes in an Antiglioma Activity. It has been shown that T cells in GBM patients exhibit an exhaustion phenotype characterized by the expression of PD1/TIM3/Lag3 (8, 57, 58). Our analysis of patients' peripheral lymphocytes and TILs indicates cells that are positive for all exhaustion markers (triple-positive cells) comprise 5.48 ± 4.8% of PB $PD1^+CD8s$ and 7.67 ± 3.87 of $PD1^+$TILs (Fig. 3 *A* and *B*). Low-level expression of activation markers CD69 and CD25 was detected in $CD8^+$ cells (Fig. 3 *C* and *D*). In addition, flow cytometry analysis showed that 35.68 ± 5.21% of PB CD8s and 28.99 ± 5.218% of TILs isolated from patients' tissues are positive for IFNγ (*SI Appendix*, Fig. S3*A*). The average number of $TNFα^+$ cells within the PB CD8s and TILs was 1.83 ± 0.7% and 8.67 ± 6.17%, respectively (*SI Appendix*, Fig. S3*B*).

We processed blood and tissues from two GBM patients and found that PB and TILs could be stimulated for antiglioma activity when cocultured with $IL13Rα2^+$ GBMs in the presence of $BiTE^{LLON}$, but not $BiTE^{LLOFF}$ (Fig. 3 *E* and *F*). The potency of TILs cocultured with $BiTE^{LLON}$ in killing GBM cells was variable between patients in relation to bead-stimulated cells.

PB and TIL cocultured with GBM cells showed activation and increased expression of PD-1 at the cell surface (Fig. 3*G* and *SI Appendix*, Fig. S3 *C* and *D*). There was also an increase of triple+ peripheral lymphocytes and TILs after $BiTE^{LLON}$ and bead stimulation, but not when treated with $BiTE^{LLOFF}$ or in unstimulated conditions ($BiTE^{LLON}$: PB CD8 triple+ 13.52 ± 6.38% and TILs triple+ 20.52 ± 9.98%; Stimulated: PB CD8 triple+ 28.03 ± 17.45% and TILs triple+ 35.15 ± 1.66%) (Fig. 3*H*).

$BiTE^{LLON}$ induced significantly more $IFNγ^+$ PB CD8 cells, as compared to $BiTE^{LLOFF}$ or unstimulated cells ($P < 0.0001$) (Fig. 3 *I* and *J*). In stratifying cells according to exhaustion markers, we determined that contributors to the production of IFNγ in $BiTE^{LLON}$-stimulated cultures are distributed within all exhaustion marker subtypes, with $PD1^+Lag3^+$ cells comprising the largest subgroup (46.53 ± 1.7%) (*SI Appendix*, Table S2). In positive control PB coculture (activated with beads), $PD\text{-}1^+$ cells were determined as the major producers of IFNγ (*SI Appendix*, Table S2). The profile of TNFα in cocultured PB lymphocytes was similar to the IFNγ (*SI Appendix*, Fig. S3 *E* and *F*).

Patient TILs secreted significantly more IFNγ when cocultured with $BiTE^{LLON}$ than negative controls and bead-stimulated cells ($P < 0.005$) (Fig. 3*K*). Flow cytometry analysis also showed a higher expression of $IFNγ^+$ in TILs when cultured with $BiTE^{LLON}$ as compared to negative controls, but not to bead-activated cultures (Fig. 3*L*). When stratified by individual exhaustion phenotypes, triple+ TILs were the most significant contributors to IFNγ in $BiTE^{LLON}$- and bead-stimulated culture conditions (*SI Appendix*, Table S2). Flow cytometry analysis revealed that $BiTE^{LLON}$ causes an increase in TIL intracellular TNFα (*SI Appendix*, Fig. S3*G*). The most significant contributors to the pool of $TNFα^+$ cells were triple+ TILs (*SI Appendix*, Table S2).

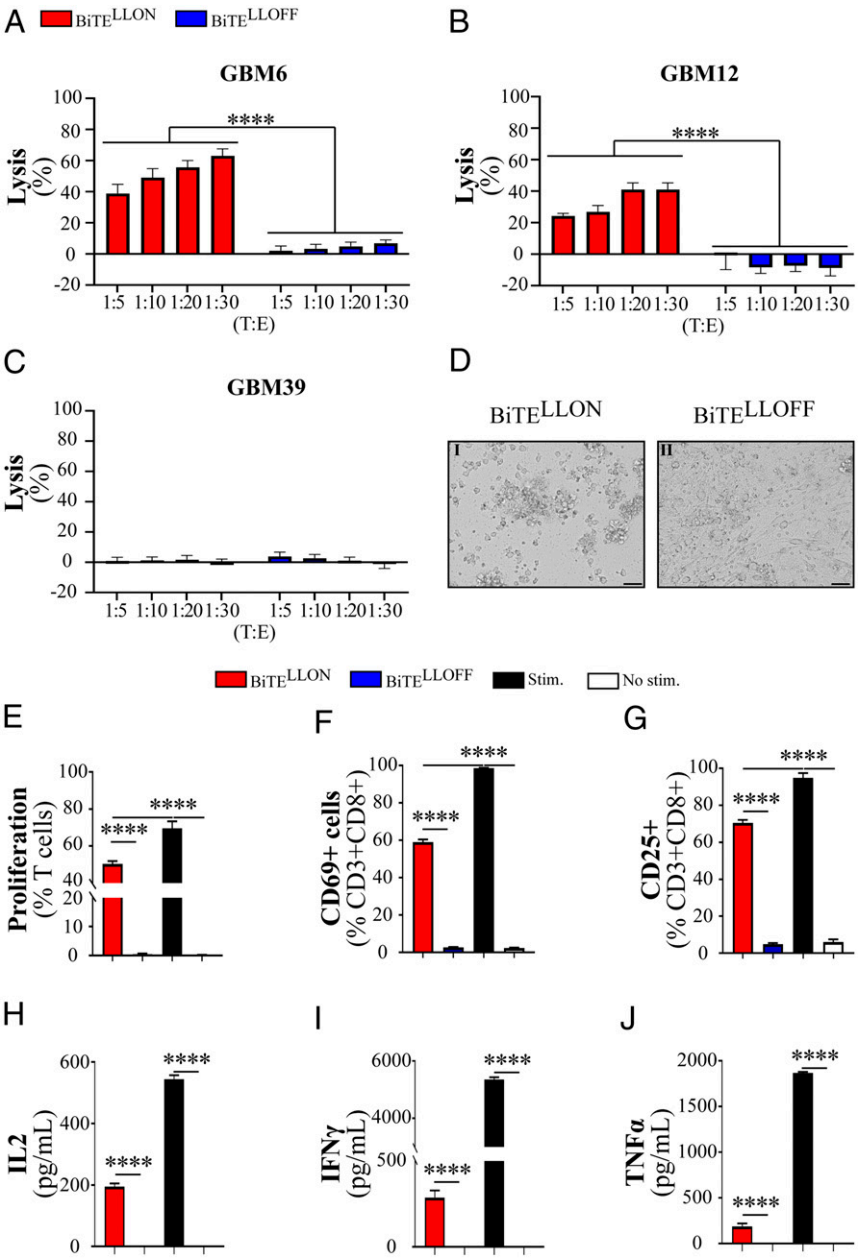

Fig. 2. BiTE^{LLON} activates T cell and induces the killing of IL13Rα2^{+} gliomas. Chromium 51 (^{51}Cr) release assay shows that (*A*) GBM6 and (*B*) GBM12 are killed by donor T cells in the presence of BiTE^{LLON}, but not BiTE^{LLOFF}, in all tested target-to-effector (T:E) ratios (two-way ANOVA, $n = 4$, $^{****}P < 0.0001$). (*C*) GBM39 gliomas are spared by donor T cells in the presence of either BiTE^{LLON} or BiTE^{LLOFF}. (*D*) Bright-field pictures of T cells with IL13Rα2-expressing GBMs after 3 d in coculture in the presence of BiTE^{LLON}(*I*) and BiTE^{LLOFF}(*II*) (Scale bar: 50 μm.). (*E*) Proliferation and expression of activation markers (*F*) CD69 and (*G*) CD25 after coculture of donor T cells for 3 d with BiTE^{LLON}, BiTE^{LLOFF}, stimulation with CD2CD3CD28 beads (Stim.) or absence of any form of stimulation (No stim.) with GBM12 gliomas (one-way ANOVA, $n = 3$, $^{****}P < 0.0001$). ELISA for the production of (*H*) IL2 (24 h), (*I*) IFNγ (48 h), and (*J*) TNFα (48 h) by T cells after coculture with GBM12 in the presence of BiTE^{LLON}, BiTE^{LLOFF}, stimulation with CD2CD3CD28 beads (Stim.), or absence of any form of stimulation (No stim.) (one-way ANOVA, $n \geq 4$, $^{****}P < 0.0001$).

Altogether, these data show that BiTE^{LLON} stimulates anti-glioma activity in patient T cells and induces cytokine production in triple exhausted TILs.

Development of NSCs Secreting Functional BiTE. BiTEs can cross the BBB, but the rate at which they are degraded and cleared from the body necessitates repeated systemic administration in cancer patients (35, 59). We and others have demonstrated that NSCs can migrate in the brain toward GBM cells/tissue and produce therapeutic antibodies for extended periods of time (60–62). For this study, we modified immortalized NSCs (63–65) for BiTE^{LLON} and BiTE^{LLOFF} synthesis and secretion (*SI Appendix*, Fig. S4*A*) (60). Modified NSCs were fluorescence-activated cell sorter (FACS) sorted by their expression of the ZsGreen1 reporter (Fig. 4*A*). Cytogenic studies of NSCs modified for synthesis and secretion of BiTE^{LLON} (NSC^{LLON}) showed the same karyotype as the parental NSCs (*SI Appendix*, Fig. S4*B*). Results from immunocytochemical analysis (Fig. 4 *B* and *C*) and Western blotting (Fig. 4*D*) showed that NSC^{LLON} and NSC^{LLOFF} produce BiTE protein. BiTEs secreted by NSC^{LLON}, but not NSC^{LLOFF},

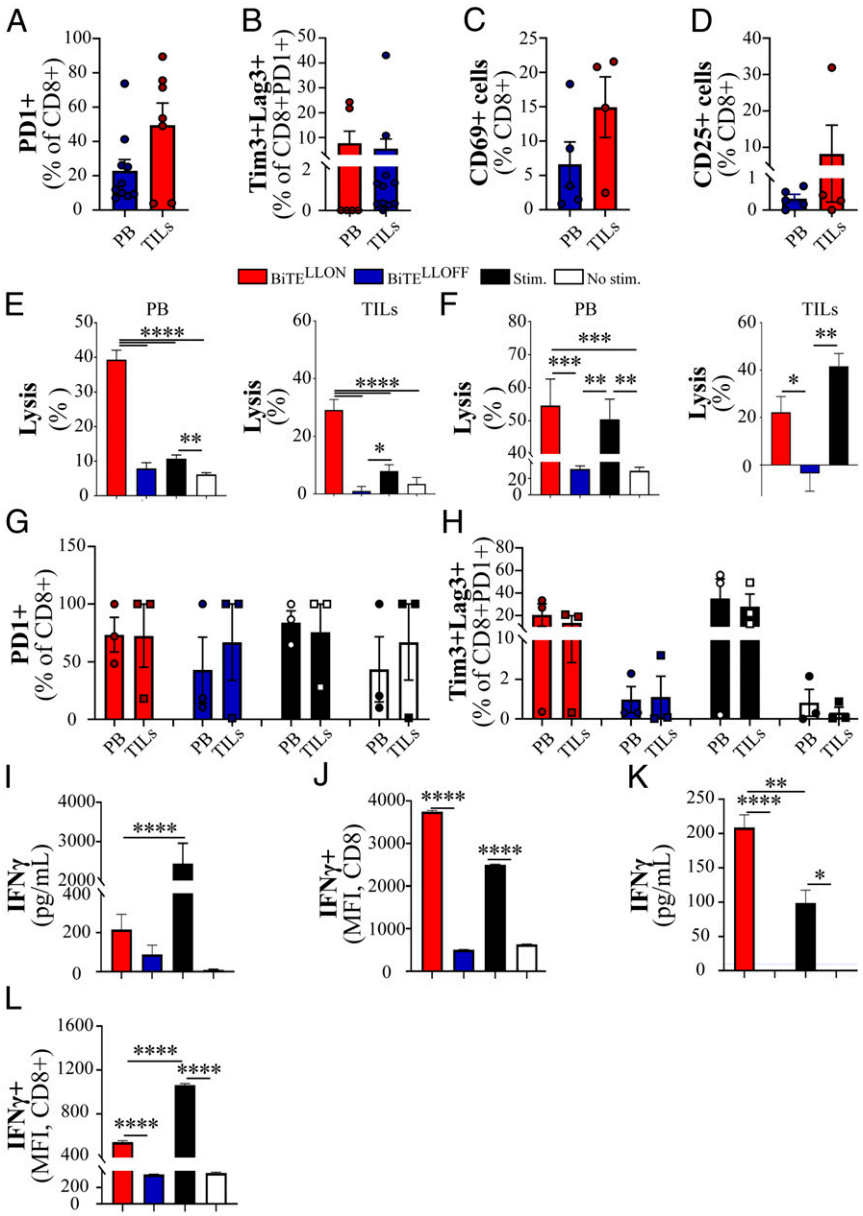

Fig. 3. BiTE^{LLON} engages GBM patients' lymphocytes in an antiglioma activity. Basal levels of (*A*) PD-1, exhaustion markers (*B*) PD1, Lag3, Tim3, and activation markers (*C*) CD69, (*D*) CD25, in cells isolated from PB and TILs as evaluated by flow cytometry ($n \geq 7$). GBM12 ^{51}Cr killing assay determined the reengagement of PB and TILs from GBM (*E*) patient 1 and (*F*) patient 2 into glioma killing in the presence of BiTE^{LLON} and CD2CD3CD28 beads (Stim.), but not BiTE^{LLOFF} or not stimulation (No stim.) (one-way ANOVA, $n \geq 2$, $^{*}P < 0.05$, $^{**}P < 0.01$, $^{***}P < 0.001$, $^{****}P < 0.0001$). Flow cytometric analysis of (*G*) PD-1 and (*H*) PD-1, Tim3, and Lag3 after coculture for 3 d of PB lymphocytes or TILs with IL13Rα2-expressing gliomas ($n = 3$). Evaluation of (*I*) secreted (ELISA) and (*J*) intracellular (flow cytometry) levels of IFNγ in lymphocytes isolated from GBM patients' PB (one-way ANOVA, $n = 2$–12, $^{*}P < 0.05$, $^{**}P < 0.01$, $^{****}P < 0.0001$). Secreted (*K* and *L*) intracellular (flow cytometry) levels of IFNγ in TILs isolated from GBM patients (one-way ANOVA, $n = 2$–3, $^{*}P < 0.05$, $^{**}P < 0.01$, $^{****}P < 0.0001$).

showed strong binding to human recombinant IL13Rα2 (hrIL13Rα2) immobilized on ELISA plates (Fig. 4*E*). Quantitative analysis revealed that 1×10^6 of NSC^{LLON} produced 1.6 ± 0.13 μg of BiTE within the first 24 h and 2.42 ± 0.26 μg after an additional day in culture (48 h) (Fig. 4*F*). NSC^{LLON} and NSC^{LLOFF} are tropic for GBM cells in vitro (Fig. 4*G* and *SI Appendix*, Fig. S4*C*).

Iron-labeled NSC^{LLON} (Fig. 4*H* and *SI Appendix*, Fig. S4 *D* and *E*) were followed by MRI for 5 d after injection into the hemisphere contralateral to the tumor-bearing brain of animal subjects (*SI Appendix*, Fig. S4*F*), as previously described (62). T2* (effective T2) weighted MRI signal showed NSC^{LLON} accumulation in the tumor-bearing hemisphere that reached a maximum level at 24 to 48 h after injection (Fig. 4*I* and *SI Appendix*, Fig. S4 *G* and *H*). The signal from the hemisphere injected with NSC^{LLON} (contralateral to the tumor-bearing hemisphere) was highest at 3 h after injection and progressively decreased after that (Fig. 4*I*). Quantitative analysis of R2* data (where R2* is 1/T2*), revealed maximal tumor coverage by NSC^{LLON} within 48 h from the intracranial injection of cells ($P = 0.0063$) (Fig. 4*J* and *SI Appendix*, Fig. S4*G*).

NSCs could be immunosuppressive or immunoreactive due to the presence of MHCI and PDL-1 at their cell surface (*SI Appendix*, Fig. S5*A*) (66, 67). NSCs express MHCI on the surface

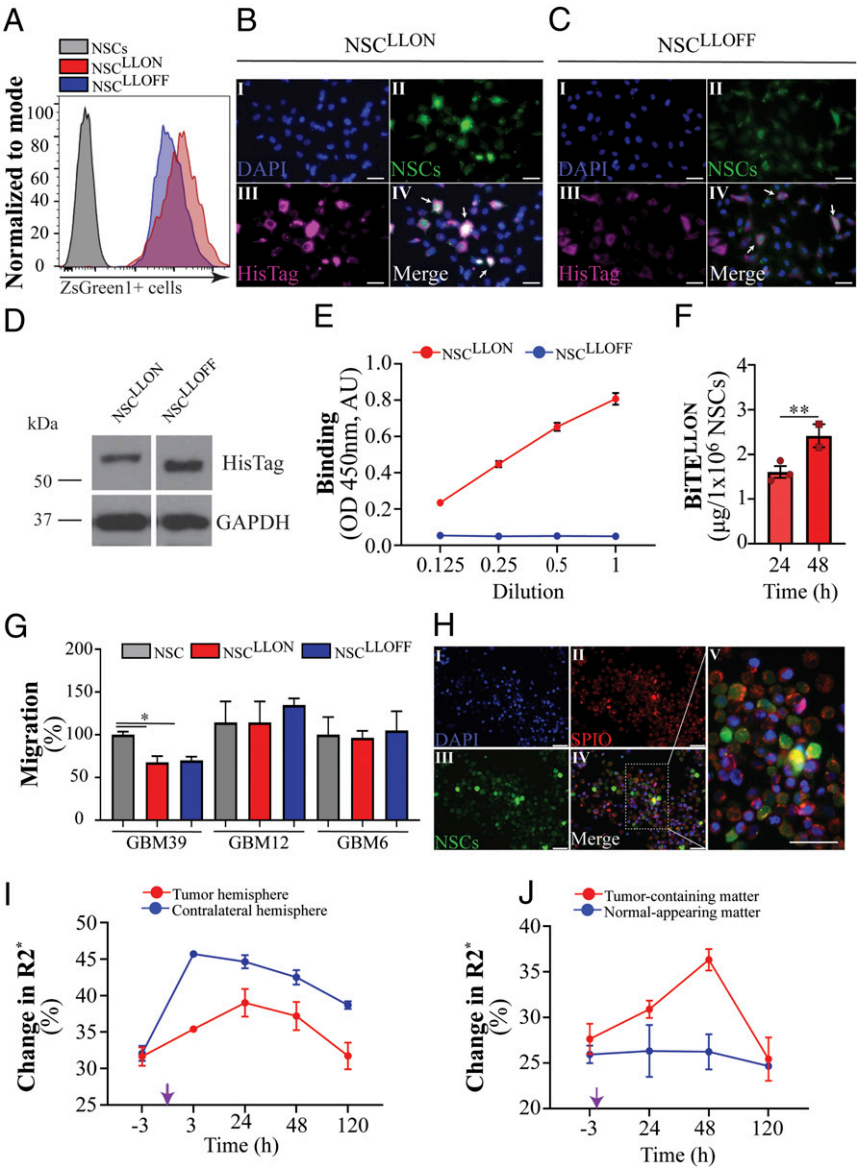

Fig. 4. NSCs produce and deliver BiTE^{LLON} protein to tumors in vivo. BiTE-transduced NSCs were sorted for the expression of (*A*) ZsGreen1 (sample histogram) protein and evaluated for the production of BiTE proteins using immunocytochemistry by (*B*) NSC^{LLON} and (*C*) NSC^{LLOFF} cells immobilized on cover glass (cells-DAPI-nucleus [*I*], NSC-ZsGreen1 [*II*], BiTE protein-α-His-Tag [*III*], and [*IV*] merged together. (Scale bars: 50 µm.) (*D*) Western blotting using anti-His Tag and anti–glyceraldehyde-3-phosphate dehydrogenase (anti-GAPDH) antibodies. (*E*) NSC^{LLON} but not NSC^{LLOFF} produced protein binding to IL13Rα2 protein immobilized on ELISA plates. (*F*) Production dynamics of BiTE^{LLON} by NSC^{LLON} after 24 and 48 h in culture (*t* test, $n = 3$, $^{**}P < 0.01$). (*G*) Migratory capacity of parental (NSCs) and modified NSC^{LLON} and NSC^{LLOFF} toward conditioned media collected from human xenograft cell lines GBM39, GBM12, and GBM6 cultured in vitro was assessed in invasion chambers (one-way ANOVA, $n = 3$, $^{*}P < 0.05$). (*H*) Immunocytochemical analysis of NSC^{LLON} labeled with superparamagnetic iron oxide contrast (SPIO) particles used for dynamic in vivo tracking of NSCs by MRI. Scale bar, 50 µm. (*I*) Labeled NSC^{LLON} injected into a contralateral hemisphere, robustly egressed from the injection site, and migrated toward the tumor. The change in the NSC^{LLON} movement within the brain is expressed as a change in R2*, a signal corresponding to labeled NSCs ($P = 0.0005$ as described in *SI Appendix, Statistics and data analysis*) and achieved (*J*) maximum tumor coverage within 2 d ($P = 0.0063$). Purple arrow, injection time point = 0 h. AU, arbitrary units.

(*SI Appendix*, Fig. S5*A*). Profiling for checkpoint molecules showed that 20.02 ± 2.26% of NSC^{LLON} and 39.57 ± 3.9% of NSC^{LLOFF} expressed a low level of PD-1 ligand (PDL-1) at the cell surface (*SI Appendix*, Fig. S5 *B–D*). Modified NSCs do not express PDL-2 or cytotoxic T lymphocyte-associated protein 4 (CTLA4) (*SI Appendix*, Fig. S5 *C* and *D*). The presence of PDL-1 did not affect secreted BiTE^{LLON} from promoting a strong T cell antiglioma response (NSCs vs. NSC supernatant) (*SI Appendix*, Fig. S5*E*).

NSC^{LLON}, but not BiTEs from NSC^{LLOFF}, produced BiTE that potently stimulates donor's lymphocytes, leading to the killing of IL13Rα2-positive GBM cells (Fig. 5 *A* and *B*). NSC^{LLON} and NSC^{LLOFF} did not induce lymphocyte killing of IL13Rα2-negative cells (Fig. 5*C*). GBM patient lymphocytes were also activated against GBM cells by NSC^{LLON} (Fig. 5*D*). NSC^{LLON}, but not NSC^{LLOFF}, up-regulated lymphocyte expression of granzyme B (GrzmB) and Lamp1, markers of degranulation, and mediators of the perforin-associated killing of IL13Rα2^{+} GBM cells. These effects were not observed in the absence of IL13Rα2 (Fig. 5*E*). BiTEs secreted by the NSC^{LLON} also induced lymphocyte proliferation (Fig. 5*F*), activation (Fig. 5 *G* and *H*), and production of type 1 cytokines: IL2, IFNγ,

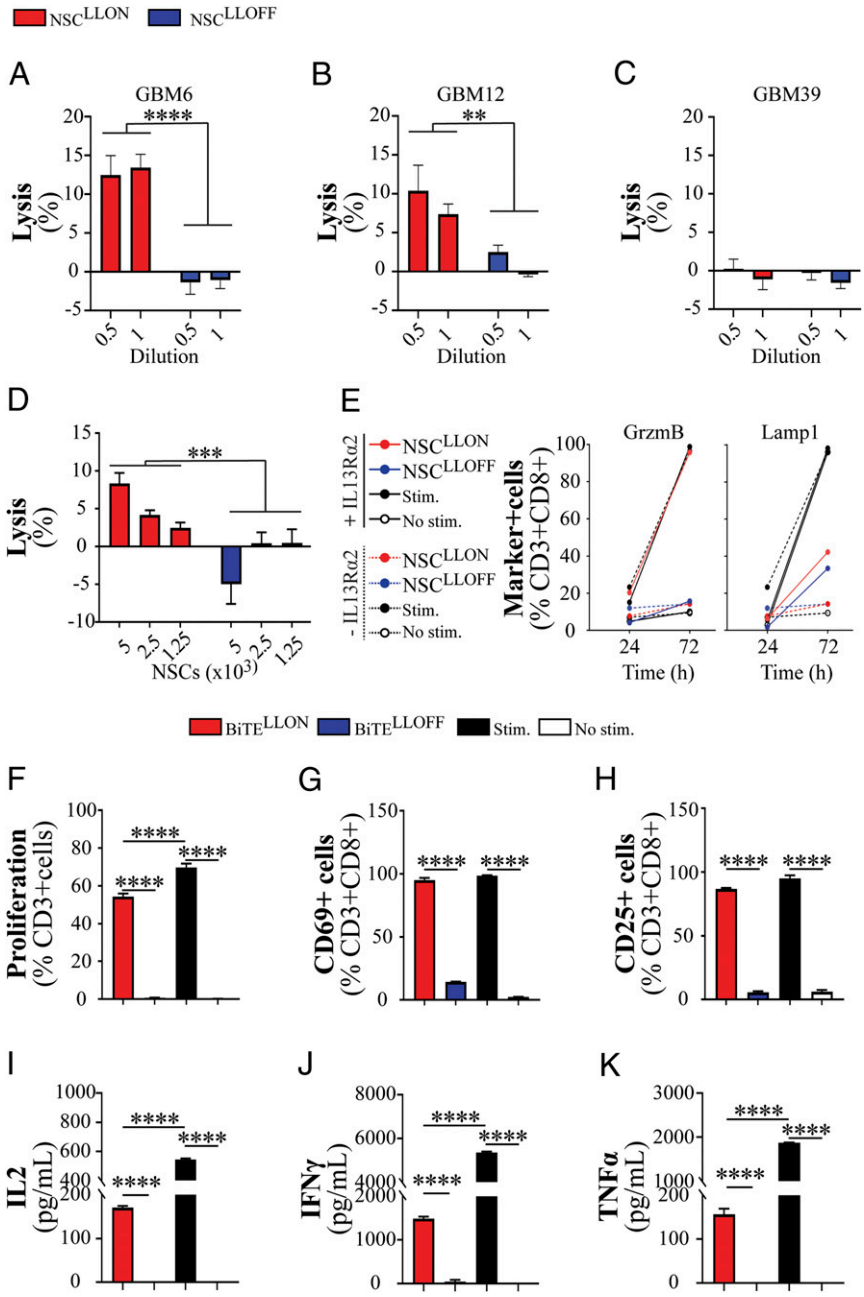

Fig. 5. BiTE^{LLON} secreted by NSCs is functional in vitro. NSC^{LLON} produce BiTE protein that induced a robust killing in two IL13Rα2^{+} cell lines, (*A*) GBM6 and (*B*) GBM12 (two-way ANOVA, $n = 4$, $^{**}P < 0.01$, $^{****}P < 0.0001$). (*C*) BiTE secreting NSCs did not engage donor T cells to kill GBM39, an IL13Rα2-negative cell line. (*D*) NSC^{LLON} presence in a coculture, but not NSC^{LLOFF}, induced GBM patient's T cells' reengagement to kill GBM12 cells (two-way ANOVA, $n = 3$, $^{***}P < 0.001$). (*E*) Coculture of donor T cells with GBM12 in the presence of NSC^{LLON} and bead stimulation, but not NSC^{LLOFF} or absence of stimulation, induced expression of Granzyme B (GrzmB) and Lamp1 (markers of cytotoxic T cell activity), (*F*) proliferation and expression of activation markers (*G*) CD69 and (*H*) CD25 in T cells (one-way ANOVA, $n \geq 3$, $^{****}P < 0.0001$). Activation of T cells was associated with the production of (*I*) IL2 (24 h), (*J*) IFNγ (48 h), and (*K*) TNFα (48 h) by T cells after coculture with GBM12 in the presence of BiTE^{LLON} or stimulation with CD2CD3CD28 beads (Stim.), but not in BiTE^{LLOFF} or absence of any form of stimulation (No stim.) (one-way ANOVA, $n \geq 4$, $^{****}P < 0.0001$).

and TNFα (Fig. 5 *I–K*) in cocultures with IL13Rα2-positive GBM cells (Fig. 5 *F–K* and *SI Appendix*, Fig. S5 *F–K*).

NSC^{LLON} Administration Extends the Survival of Glioma-Bearing Animals. We injected NSC^{LLON} proximally (1.5 mm) to GBM12 intracranial tumors in NSG mice (*SI Appendix*, Fig. S6*A*). Immunohistochemical analysis of sections of brains harvested on days 3 and 7 following NSC^{LLON} injection showed robust infiltration of the tumor mass by stem cells and the production of BiTE protein within the tumor and at the tumor periphery (Fig. 6*A* and *SI Appendix*, Fig. S6 *B* and *C*). We also evaluated NSC^{LLON} for the duration of in vivo viability by histopathologic analysis of resected mouse brains from animal subjects euthanized at 90 d following NSC^{LLON} injection (*SI Appendix*, Fig. S7 *A–C*), with GBM12 serving as a positive control. There were no Ki67-positive (e.g., proliferating) cells found in the mouse brain injected with NSC^{LLON}, in contrast to the brain with GBM12 tumors (*SI Appendix*, Fig. S7*B*). Only a few NSC^{LLON}

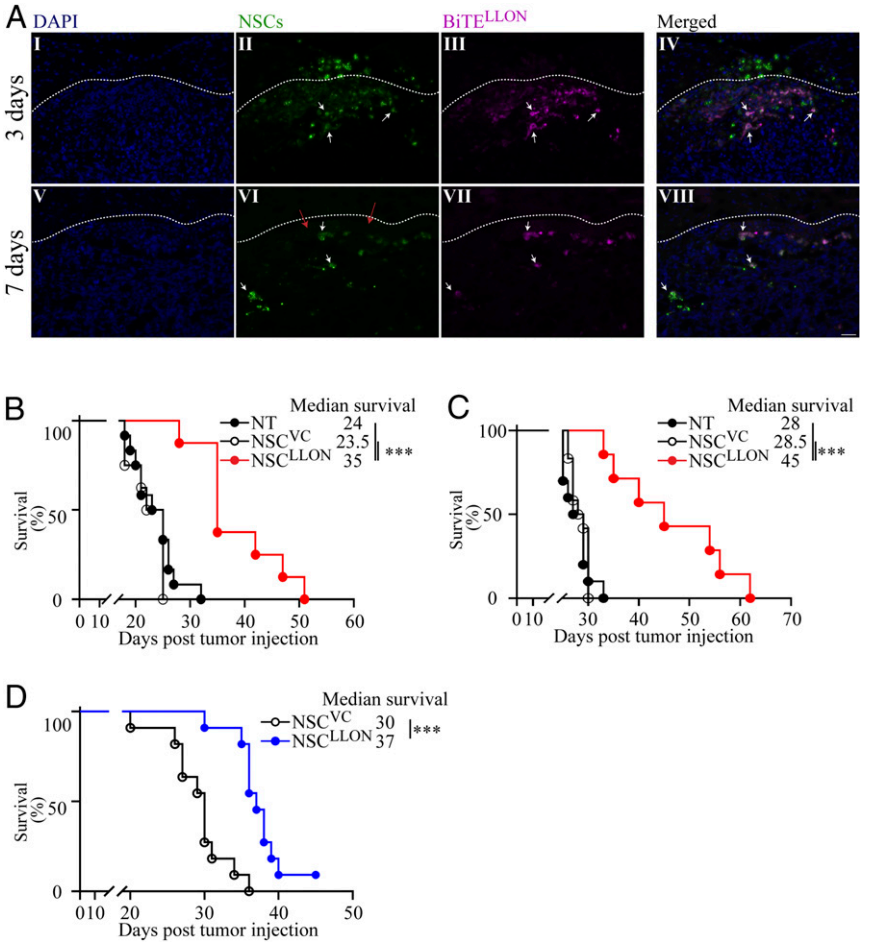

Fig. 6. NSC^{LLON} treatment significantly extends the survival of glioma-bearing animals. (*A*) NSC^{LLON} injected superior and 1.5 mm proximal to the tumor mass (for large magnification and orientation concerning NSC^{LLON} injection, please see *SI Appendix*, Fig. S6) persist for an extended time, infiltrate tumor mass (direction of infiltration is shown with red arrows), and secrete therapeutic proteins in situ (dotted line marks the tumor edge, DAPI cells, blue; NSCs, green; BiTE^{LLON}, magenta; *I–IV*, 3 d and *V–VIII*, 7 d after injection; NSCs and BiTE expression are shown with white arrows) (Scale bar: 50 μm). (*B–D*) Animals bearing IL13Rα2-expressing gliomas (1.0×10^5 GBM6 or GBM12) were treated with a single intracranial (i.c.) injection of 1×10^6 NSC^{LLON} and PB cells, either at the tumor mass i.c. (red, 1.5×10^6 PB) or injected intravenously (i.v.) (blue, 7×10^6 PB). (*B*) GBM12-bearing animals treated with NSC^{LLON} and PB i.c. survived significantly longer than not treated (NT) or treated with NSC^{VC} and PB (Kaplan–Meier survival curves were compared using log-rank tests, $P < 0.0001$, and adjusted for *P* values using the Holm–Sidak method: NT vs. NSC^{VC} $P = 0.31$, NSC^{VC} vs. NSC^{LLON} $^{***}P = 0.0003$, $n = 8$). (*C*) Similarly, treated mice transplanted with GBM6 cells survived significantly longer from the control NSC^{VC} or NT animals (Kaplan–Meier survival curves were compared using log-rank tests, $P = 0.0002$, and adjusted for *P* values using the Holm–Sidak method: NT vs. NSC^{VC} $P = 0.54$, NSC^{VC} vs. NSC^{LLON} $^{***}P = 0.0009$, $n \geq 8$). (*D*) GBM6-bearing mice treated with an i.c. NSC^{LLON} and i.v. PB lived significantly longer than mice transplanted with control NSC^{VC} and i.v. PB animals (Kaplan–Meier survival curves were compared using log-rank tests, $^{***}P < 0.001$, n = 11).

cells were detected near the third ventricle, but not in other brain regions (*SI Appendix*, Fig. S7*C*). Moreover, implantation of NSC^{LLON} in tumor-bearing mice in the absence of T cells did not affect the tumor progression compared to untreated control mice in GBM12- and GBM39-bearing mice (GBM12 median survival: not treated [NT], 22 d; NSC^{LLON}, 26 d; log-rank test, $P = 0.269$) (*SI Appendix*, Fig. S7*D*) (GBM39 median survival: NT, 84.5 d; NSC^{LLON}, 71 d; log-rank test, $P = 0.095$) (*SI Appendix*, Fig. S7*E*). Interestingly, the ex-vivo analysis of GBM6 and GBM12 glioma cells harvested from brain xenografts showed a much smaller fraction of glioma cells expressing IL13Rα2 (*SI Appendix*, Fig. S7 *F* and *G*) in comparison to GBM6 and GBM12 cells cultured in vitro (Fig. 1 *E* and *F*). Infiltration of NSC^{LLON} into the tumor mass with the accompanied secretion of BiTE^{LLON} could be detected in tumors 3 d after NSC^{LLON} injection (Fig. 6 *A*, *II*, *III*, and *IV* and *SI Appendix*, Fig. S6*B*). Both NSCs and BiTE were also detectable in the tumor at day 7 postinjection, albeit at lower levels (Fig. 6 *A*, *II* vs. 6 *A*, *VI* and Fig. 6 *A*, *III* vs. 6 *A*, *VII*).

We treated GBM12-bearing mice by intratumoral injection with either NSC^{LLON} or NSC vector control (NSC^{VC}) and PB lymphocytes (Fig. 6*B*). Treatment with NSCs secreting therapeutic BiTEs increased average animal survival by 67%. Animals bearing GBM6 tumors were treated using the same protocol as for GBM12-bearing animals (Fig. 6*C*). GBM6-bearing mice treated with NSC^{LLON+} PB lived on average 63.3% longer than animals that were NT or those that received an injection of NSC^{VC+} PB . In contrast to GBM6 and GBM12, treatment of mice bearing IL13Rα2-negative GBM39 tumors with NSC^{LLON} and PB did not extend animals' survival compared to the NT group (*SI Appendix*, Fig. S7*E*). Animals bearing GBM6 tumors and treated with intratumoral injection of NSC^{LLON} but an intravenous infusion of PB also survived significantly longer than mice treated with control NSC^{VC} (Fig. 6*D*). Histopathologic analysis of brains from the control and treated animals showed the absence of therapy-related toxicity, including demyelination, encephalomyelitis, or neuronal loss.

Altogether, these data show that NSCs secreting BiTE^{LLON} deliver a sustained therapeutic protein source for local engagement of CD3$^+$ cells for an antiglioma activity.

Discussion

This study reports the development and functional analysis of NSCs secreting novel proteins that stimulate patient-derived T cell antitumor activity in vitro and in vivo. We show that IL13Rα2-targeted BiTEs, secreted by NSC^{LLON}, promote T cell killing of IL13Rα2$^+$ tumor cells by engaging the tumor cell antigen target with T cell CD3ε. The genetically modified NSCs produce and secrete BiTE in vivo while infiltrating the tumor mass, with treated animals bearing intracranial tumors experiencing significant survival benefit.

Demonstration of target specificity is essential for limiting undesirable side effects from BiTE treatment of cancer patients (30, 32, 44, 68), and, for this reason, we have developed BiTE targeting IL13Rα2 (51, 52). We show BiTE^{LLON} binding specificity for PDX cells expressing IL13Rα2 and T cell CD3ε, with this dual binding specificity promoting T cell-mediated cell death to IL13Rα2-positive tumor cells. The absence of cell killing in T cell–tumor cell cocultures with nonbinding BiTE^{LLOFF}, and in cocultures where tumor cells lack the IL13Rα2 antigenic target, supports the specificity of BiTE^{LLON}. Maximal BiTE antitumor activity was observed at a concentration of 2.5 μg/mL and a T:E cell ratio (1:5), suggesting that relatively low amounts of recombinant protein are needed for antineoplastic effect (43).

Prolong T cells' stimulation results in the expression of activation markers PD-1, Tim3, Lag3, and T cell exhaustion (69, 70). GBMs are known to suppress lymphocyte activation processes and promote T cell exhaustion characterized by T cell expression of PD-1, Tim3, and Lag3 (57, 58). Our results show that BiTE^{LLON} activates patient-derived peripheral and tumor-infiltrating T cells to kill IL13Rα2$^+$ GBMs, irrespective of T cell expression of these proteins.

It has been shown that activation of T cells by targeted immunotherapeutics can lead to aberrant cytokine production and cytokine release storm (CRS) in treated patients (44, 71). In our study, donor T cells stimulated directly with BiTE^{LLON}, or by BiTE^{LLON} secreted by NSCs, produced IFNγ and TNFα, but only in the presence of IL13Rα2-expressing tumor cells. Interestingly, we found that CD8$^+$ T cells, positive for PD-1, Tim3, and Lag3, are major contributors to the pool of secreted cytokines when treated with BiTE^{LLON}, while in the presence of IL13Rα2-expressing cells. Notably, BiTE^{LLON} successfully activated both PB lymphocytes and TIL cells against IL13Rα2-expressing tumor in cases when T cells were harvested from patients receiving steroid treatment, which is known to suppress T cell activity (72, 73).

Unlike blood vessels of a healthy brain, GBM vasculature is considered to be disorganized and leaky, allowing larger molecules to pass from circulation to tumor tissue. Indeed, systemically delivered BiTEs, directed against the tumor-associated antigen epidermal growth factor variant III (EGFRvIII), were shown to reach the intracranial tumor in an amount that was sufficient to reduce tumor burden (74). Nonetheless, it is expected that the systemic administration of BiTE for treating GBM would require repeated treatments. Interventions such as focused ultrasound transiently opening the blood–tumor barrier (74) might be an option to improve the delivery of therapeutic protein to GBM. An approach that would potentially circumvent the need for repeated administrations is to deliver treatment locally and using a platform for sustaining therapeutic presence. To achieve this, we have investigated direct intracranial administration of BiTE-secreting NSCs. Therapeutic NSCs' migration toward and dissemination within brain tumors in mice, following systemic and intracranial NSCs' administration routes, have been previously demonstrated by our group and colleagues (67, 74, 75). In the current study, intracranially administered NSC^{LLON} show tropism to and dissemination within glioma xenografts. Our results also show that NSC^{LLON} persist and secrete BiTE for at least 7 d following administration, thereby extending the supply of BiTE within the tumor. Others have reported the persistence of engineered human NSCs in a mouse brain for up to 12 wk (74). Nevertheless, it is anticipated that there will be a decrease in the number of NSCs within the tumor over time, as indicated by MRI (Fig. 4 *I* and *J* and *SI Appendix*, Fig. S4*G*). This results in decreased levels of locally secreted BiTEs, contributing to this therapy's limited antitumor efficacy. Sustained or repeated delivery of therapeutic NSCs to brain tumor patients, using already clinically available methods, such as an Ommaya reservoir placement, would presumably extend treatment benefit.

The drawback of many targeted therapies against tumors is antigen escape (27, 28, 49), necessitating the development of therapeutics to multiple targets. This is partly due to the heterogeneous expression of TAA, including IL13Rα2, in GBM tissue (28, 55, 75). In our experimental models, only a fraction of GBM12 and GBM6 cells express IL13Rα2 in vivo, recapitulating the pattern of antigen expression in GBM. Thus, treatment-associated selection against TAA-positive cells is another factor that would likely limit the therapeutic efficacy of any BiTE therapy directed to a single tumor antigen. Antigen escape in tumors treated with CAR T cells directed to a single target has been demonstrated in preclinical and clinical GBM studies (27, 28, 49). The CAR T cells secreting BiTEs have recently been investigated as a platform for targeting multiple tumor antigens (48). However, the short life of CAR T cells in the tumor environment is expected to translate into a similarly short presence of BiTEs produced by T cells. Stem cells engineering strategy or loading NSCs with vectors encoding for multispecific molecules could overcome the limitations mentioned above. The oncolytic virus expressing BiTE, cytokine, and checkpoint blockade has been generated and tested in combination with CAR T cells (76). A multifunctional vector delivered to the tumor by NSCs will ensure a robust intratumoral distribution of therapeutic molecules.

Tumor inhibition of T cell function through an aberrant expression of immune checkpoint proteins and tumor MHC downregulation is a critical mechanism by which GBM escapes antitumor immune response (39, 57, 58). Based on this knowledge, immune-checkpoint inhibitor (3) therapy has been tested in clinical trials. However, the results have shown a lack of survival benefit for treated GBM patients (3, 77–79). Based on the results presented here, it would be interesting to compare the antitumor activity of local NSC^{LLON} administration in combination with systemically or locally delivered checkpoint inhibitors. Interestingly, a BiTE molecule engineered to interact with T cells and PD-L1 has been recently tested in preclinical models of PD-L1–positive tumors, with results showing extended survival of treated animal subjects (80). Based on these findings and results presented here, one can envision a scenario in which multiple types of modified NSCs, each producing BiTEs that target distinct tumor antigens, were used in treating GBM patients.

It is relevant to consider shortcomings associated with animal models that lack a fully functional immune system and, therefore, have an inherent deficiency in recapitulating the tumor microenvironment of a GBM. Future studies utilizing immunocompetent hosts will be necessary for revealing BiTE interactions with a fully functional host immune system (81). The use of humanized mouse models, in which mice have been modified for durable production of human immune cells, or the use of genetically engineered mice that express the human CD3 receptor, will also be of interest.

Thus, the current study represents a starting point for expanding the investigation of BiTEs produced by genetically modified NSCs,

for treating GBM. The results we have in hand are encouraging and merit continued exploration of this therapeutic modality.

Materials and Methods

For a detailed description of cell lines, generation of BiTE molecules and NSCs secreting BiTEs, functional in vitro assays, flow cytometry, immunocytochemistry, animal tumor, and MRI studies, statistics, and data analysis, please see *SI Appendix, Materials and Methods*.

Data Availability. All study data are included in the article and/or *SI Appendix*.

ACKNOWLEDGMENTS. This research was supported by NIH Grants R33NS101150 (to I.V.B.), R01NS106379 (to I.V.B.), and P50CA221747 (to M.S.L.). The Northwestern Nervous System Tumor Bank is supported by the P50CA221747 Specialized Program of Research Excellence for Translational Approaches to Brain Cancer. Histology services were provided by the Northwestern University Mouse Histology and Phenotyping Laboratory, which is supported by National Cancer Institute Grant P30-CA060553 awarded to the Robert H. Lurie Comprehensive Cancer Center. We thank Dolonchampa Maji, Ph.D. (Department of Neurological Surgery), Sergii Pshenychnyi, Ph.D. (the Recombinant Protein Production Core), and the Small Animal Imaging Facility at Northwestern University for assistance with this project.

1. R. Stupp *et al*., Effect of tumor-treating fields plus maintenance temozolomide vs maintenance temozolomide alone on survival in patients with glioblastoma: A randomized clinical trial. *JAMA* **318**, 2306–2316 (2017).
2. S. Ostermann *et al*., Plasma and cerebrospinal fluid population pharmacokinetics of temozolomide in malignant glioma patients. *Clin. Cancer Res.* **10**, 3728–3736 (2004).
3. J. Zhao *et al*., Immune and genomic correlates of response to anti-PD-1 immunotherapy in glioblastoma. *Nat. Med.* **25**, 462–469 (2019).
4. T. F. Cloughesy *et al*., Neoadjuvant anti-PD-1 immunotherapy promotes a survival benefit with intratumoral and systemic immune responses in recurrent glioblastoma. *Nat. Med.* **25**, 477–486 (2019).
5. K. A. Schalper *et al*., Neoadjuvant nivolumab modifies the tumor immune microenvironment in resectable glioblastoma. *Nat. Med.* **25**, 470–476 (2019).
6. A. P. Patel *et al*., Single-cell RNA-seq highlights intratumoral heterogeneity in primary glioblastoma. *Science* **344**, 1396–1401 (2014).
7. M. Martinez-Lage *et al*., Immune landscapes associated with different glioblastoma molecular subtypes. *Acta Neuropathol. Commun.* **7**, 203 (2019).
8. P. E. Fecci, J. H. Sampson, The current state of immunotherapy for gliomas: An eye toward the future. *J. Neurosurg.* **131**, 657–666 (2019).
9. T. R. Hodges *et al*., Mutational burden, immune checkpoint expression, and mismatch repair in glioma: Implications for immune checkpoint immunotherapy. *Neuro-oncol.* **19**, 1047–1057 (2017).
10. D. F. Quail, J. A. Joyce, The microenvironmental landscape of brain tumors. *Cancer Cell* **31**, 326–341 (2017).
11. J. Galon *et al*., Type, density, and location of immune cells within human colorectal tumors predict clinical outcome. *Science* **313**, 1960–1964 (2006).
12. M. E. Dudley *et al*., Adoptive cell transfer therapy following non-myeloablative but lymphodepleting chemotherapy for the treatment of patients with refractory metastatic melanoma. *J. Clin. Oncol.* **23**, 2346–2357 (2005).
13. A. Louveau *et al*., Structural and functional features of central nervous system lymphatic vessels. *Nature* **523**, 337–341 (2015).
14. X. Hu *et al*., Meningeal lymphatic vessels regulate brain tumor drainage and immunity. *Cell Res.* **30**, 229–243 (2020).
15. G. Dupont *et al*., Our current understanding of the lymphatics of the brain and spinal cord. *Clin. Anat.* **32**, 117–121 (2019).
16. S. Prasad, J. R. Lokensgard, T. Brain-Resident, Brain-resident T cells following viral infection. *Viral Immunol.* **32**, 48–54 (2019).
17. K. L. Congdon, L. A. Sanchez-Perez, J. H. Sampson, Effective effectors: How T cells access and infiltrate the central nervous system. *Pharmacol. Ther.* **197**, 52–60 (2019).
18. A. Kim *et al*., The prognostic significance of tumor-infiltrating lymphocytes assessment with hematoxylin and eosin sections in resected primary lung adenocarcinoma. *PLoS One* **14**, e0224430 (2019).
19. A. I. Hida *et al*., Diffuse distribution of tumor-infiltrating lymphocytes is a marker for better prognosis and chemotherapeutic effect in triple-negative breast cancer. *Breast Cancer Res. Treat.* **178**, 283–294 (2019).
20. C. A. Castaneda *et al*., Relationship between tumor-associated immune infiltrate and p16 staining over clinicopathological features in acral lentiginous melanoma. *Clin. Transl. Oncol.* **21**, 1127–1134 (2019).
21. M. Zengin, Prognostic role of tumour-infiltrating T lymphocytes in stage IIA (T3N0) colon cancer: A broad methodological study in a fairly homogeneous population. *Ann. Diagn. Pathol.* **41**, 69–78 (2019).
22. N. A. Rizvi *et al*., Cancer immunology. Mutational landscape determines sensitivity to PD-1 blockade in non-small cell lung cancer. *Science* **348**, 124–128 (2015).
23. S. L. Topalian *et al*., Safety, activity, and immune correlates of anti-PD-1 antibody in cancer. *N. Engl. J. Med.* **366**, 2443–2454 (2012).
24. C. Robert *et al*., Anti-programmed-death-receptor-1 treatment with pembrolizumab in ipilimumab-refractory advanced melanoma: A randomised dose-comparison cohort of a phase 1 trial. *Lancet* **384**, 1109–1117 (2014).
25. T. Powles *et al*., MPDL3280A (anti-PD-L1) treatment leads to clinical activity in metastatic bladder cancer. *Nature* **515**, 558–562 (2014).
26. S. M. Ansell *et al*., PD-1 blockade with nivolumab in relapsed or refractory Hodgkin's lymphoma. *N. Engl. J. Med.* **372**, 311–319 (2015).
27. D. M. O'Rourke *et al*., A single dose of peripherally infused EGFRvIII-directed CAR T cells mediates antigen loss and induces adaptive resistance in patients with recurrent glioblastoma. *Sci. Transl. Med.* **9**, eaaa0984 (2017).
28. C. E. Brown *et al*., Regression of glioblastoma after chimeric antigen receptor T-cell therapy. *N. Engl. J. Med.* **375**, 2561–2569 (2016).
29. M. Fossati *et al*., Immunological changes in the ascites of cancer patients after intraperitoneal administration of the bispecific antibody catumaxomab (anti-EpCAM×anti-CD3). *Gynecol. Oncol.* **138**, 343–351 (2015).
30. M. Jäger *et al*., Immunomonitoring results of a phase II/III study of malignant ascites patients treated with the trifunctional antibody catumaxomab (anti-EpCAM x anti-CD3). *Cancer Res.* **72**, 24–32 (2012).
31. H. Benonisson *et al*., CD3-Bispecific antibody therapy turns solid tumors into inflammatory sites but does not install protective memory. *Mol. Cancer Ther.* **18**, 312–322 (2019).
32. D. Goéré *et al*., Potent immunomodulatory effects of the trifunctional antibody catumaxomab. *Cancer Res.* **73**, 4663–4673 (2013).
33. M. S. Topp *et al*., Phase II trial of the anti-CD19 bispecific T cell-engager blinatumomab shows hematologic and molecular remissions in patients with relapsed or refractory B-precursor acute lymphoblastic leukemia. *J. Clin. Oncol.* **32**, 4134–4140 (2014).
34. M. Kebenko *et al*., A multicenter phase 1 study of solitomab (MT110, AMG 110), a bispecific EpCAM/CD3 T-cell engager (BiTE®) antibody construct, in patients with refractory solid tumors. *OncoImmunology* **7**, e1450710 (2018).
35. B. D. Choi *et al*., Systemic administration of a bispecific antibody targeting EGFRvIII successfully treats intracerebral glioma. *Proc. Natl. Acad. Sci. U.S.A.* **110**, 270–275 (2013).
36. M. J. Newman, D. J. Benani, A review of blinatumomab, a novel immunotherapy. *J. Oncol. Pharm. Pract.* **22**, 639–645 (2016).
37. L. Yu, J. Wang, T cell-redirecting bispecific antibodies in cancer immunotherapy: Recent advances. *J. Cancer Res. Clin. Oncol.* **145**, 941–956 (2019).
38. S. R. Frankel, P. A. Baeuerle, Targeting T cells to tumor cells using bispecific antibodies. *Curr. Opin. Chem. Biol.* **17**, 385–392 (2013).
39. D. Palesch *et al*., Cathepsin G-mediated proteolytic degradation of MHC class I molecules to facilitate immune detection of human glioblastoma cells. *Cancer Immunol. Immunother.* **65**, 283–291 (2016).
40. A. Marra, G. Curigliano, T-cell bispecific antibodies to bypass MHC class I loss in breast cancer. *Ann. Oncol.* **30**, 877–879 (2019).
41. C. Godbersen *et al*., NKG2D ligand-targeted bispecific T-cell engagers lead to robust antitumor activity against diverse human tumors. *Mol. Cancer Ther.* **16**, 1335–1346 (2017).
42. S. Ferrini *et al*., Targeting of T lymphocytes against EGF-receptor+ tumor cells by bispecific monoclonal antibodies: Requirement of CD3 molecule cross-linking for T-cell activation. *Int. J. Cancer* **55**, 931–937 (1993).
43. R. Bargou *et al*., Tumor regression in cancer patients by very low doses of a T cell-engaging antibody. *Science* **321**, 974–977 (2008).
44. F. Kroschinsky *et al*.; Intensive Care in Hematological and Oncological Patients (iCHOP) Collaborative Group, New drugs, new toxicities: Severe side effects of modern targeted and immunotherapy of cancer and their management. *Crit. Care* **21**, 89 (2017).
45. C. R. Stadler *et al*., Elimination of large tumors in mice by mRNA-encoded bispecific antibodies. *Nat. Med.* **23**, 815–817 (2017).
46. M. Compte *et al*., Tumor immunotherapy using gene-modified human mesenchymal stem cells loaded into synthetic extracellular matrix scaffolds. *Stem Cells* **27**, 753–760 (2009).
47. A. Szoor *et al*., T cell-activating mesenchymal stem cells as a biotherapeutic for HCC. *Mol. Ther. Oncolytics* **6**, 69–79 (2017).
48. B. D. Choi *et al*., CAR-T cells secreting BiTEs circumvent antigen escape without detectable toxicity. *Nat. Biotechnol.* **37**, 1049–1058 (2019).
49. G. Krenciute *et al*., Transgenic expression of IL15 improves antiglioma activity of IL13Rα2-CAR T cells but results in antigen loss variants. *Cancer Immunol. Res.* **5**, 571–581 (2017).
50. A. L. Moyano *et al*., microRNA-219 reduces viral load and pathologic changes in theiler's virus-induced demyelinating disease. *Mol. Ther.* **26**, 730–743 (2018).
51. I. V. Balyasnikova *et al*., Characterization and immunotherapeutic implications for a novel antibody targeting interleukin (IL)-13 receptor α2. *J. Biol. Chem.* **287**, 30215–30227 (2012).
52. J. W. Kim *et al*., A novel single-chain antibody redirects adenovirus to IL13Rα2-expressing brain tumors. *Sci. Rep.* **5**, 18133 (2015).
53. K. C. Pituch *et al*., Adoptive transfer of IL13Rα2-specific chimeric antigen receptor T cells creates a pro-inflammatory environment in glioblastoma. *Mol. Ther.* **26**, 986–995 (2018).
54. G. Krenciute *et al*., Characterization and functional analysis of scFv-based chimeric antigen receptors to redirect T cells to IL13Rα2-positive glioma. *Mol. Ther.* **24**, 354–363 (2016).
55. J. S. Jarboe, K. R. Johnson, Y. Choi, R. R. Lonser, J. K. Park, Expression of interleukin-13 receptor alpha2 in glioblastoma multiforme: Implications for targeted therapies. *Cancer Res.* **67**, 7983–7986 (2007).

56. B. H. Joshi, G. E. Plautz, R. K. Puri, Interleukin-13 receptor alpha chain: A novel tumor-associated transmembrane protein in primary explants of human malignant gliomas. *Cancer Res.* **60**, 1168–1172 (2000).
57. T. B. Davidson *et al*., Expression of PD-1 by T cells in malignant glioma patients reflects exhaustion and activation. *Clin. Cancer Res.* **25**, 1913–1922 (2019).
58. K. Woroniecka *et al*., T-cell exhaustion signatures vary with tumor type and are severe in glioblastoma. *Clin. Cancer Res.* **24**, 4175–4186 (2018).
59. T. H. Schaller *et al*., Pharmacokinetic analysis of a novel human EGFRvIII:CD3 bispecific antibody in plasma and whole blood using a high-resolution targeted mass spectrometry approach. *J. Proteome Res.* **18**, 3032–3041 (2019).
60. D. Kanojia *et al*., Neural stem cells secreting anti-HER2 antibody improve survival in a preclinical model of HER2 overexpressing breast cancer brain metastases. *Stem Cells* **33**, 2985–2994 (2015).
61. M. Dey *et al*., Intranasal oncolytic virotherapy with CXCR4-enhanced stem cells extends survival in mouse model of glioma. *Stem Cell Reports* **7**, 471–482 (2016).
62. D. Spencer *et al*., Pharmacologic modulation of nasal epithelium augments neural stem cell targeting of glioblastoma. *Theranostics* **9**, 2071–2083 (2019).
63. K. S. Aboody *et al*., Neural stem cells display extensive tropism for pathology in adult brain: Evidence from intracranial gliomas. *Proc. Natl. Acad. Sci. U.S.A.* **97**, 12846–12851 (2000).
64. K. S. Aboody *et al*., Neural stem cell-mediated enzyme/prodrug therapy for glioma: Preclinical studies. *Sci. Transl. Med.* **5**, 184ra59 (2013).
65. J. Portnow *et al*., Neural stem cell-based anticancer gene therapy: A first-in-human study in recurrent high-grade glioma patients. *Clin. Cancer Res.* **23**, 2951–2960 (2017).
66. D. Zhao *et al*., Neural stem cell tropism to glioma: Critical role of tumor hypoxia. *Mol. Cancer Res.* **6**, 1819–1829 (2008).
67. M. Gutova *et al*., Quantitative evaluation of intraventricular delivery of therapeutic neural stem cells to orthotopic glioma. *Front. Oncol.* **9**, 68 (2019).
68. D. Ellerman, Bispecific T-cell engagers: Towards understanding variables influencing the in vitro potency and tumor selectivity and their modulation to enhance their efficacy and safety. *Methods* **154**, 102–117 (2019).
69. K. Sakuishi *et al*., Targeting Tim-3 and PD-1 pathways to reverse T cell exhaustion and restore anti-tumor immunity. *J. Exp. Med.* **207**, 2187–2194 (2010).
70. E. J. Wherry, M. Kurachi, Molecular and cellular insights into T cell exhaustion. *Nat. Rev. Immunol.* **15**, 486–499 (2015).
71. S. S. Neelapu *et al*., Chimeric antigen receptor T-cell therapy—Assessment and management of toxicities. *Nat. Rev. Clin. Oncol.* **15**, 47–62 (2018).
72. G. D. Pountain, M. T. Keogan, B. L. Hazleman, D. L. Brown, Effects of single dose compared with three days' prednisolone treatment of healthy volunteers: Contrasting effects on circulating lymphocyte subsets. *J. Clin. Pathol.* **46**, 1089–1092 (1993).
73. M. Scudeletti *et al*., Immune regulatory properties of corticosteroids: Prednisone induces apoptosis of human T lymphocytes following the CD3 down-regulation. *Ann. N. Y. Acad. Sci.* **876**, 164–179 (1999).
74. Z. Li *et al*., L-MYC expression maintains self-renewal and prolongs multipotency of primary human neural stem cells. *Stem Cell Reports* **7**, 483–495 (2016).
75. W. Biernat, H. Huang, H. Yokoo, P. Kleihues, H. Ohgaki, Predominant expression of mutant EGFR (EGFRvIII) is rare in primary glioblastomas. *Brain Pathol.* **14**, 131–136 (2004).
76. C. E. Porter *et al*., Oncolytic adenovirus armed with BiTE, cytokine, and checkpoint inhibitor enables CAR T cells to control the growth of heterogeneous tumors. *Mol. Ther.* **28**, 1251–1262 (2020).
77. H. Guo *et al*., Deliver anti-PD-L1 into brain by p-hydroxybenzoic acid to enhance immunotherapeutic effect for glioblastoma. *J. Control. Release* **320**, 63–72 (2020).
78. D. Stanimirovic, K. Kemmerich, A. S. Haqqani, G. K. Farrington, Engineering and pharmacology of blood-brain barrier-permeable bispecific antibodies. *Adv. Pharmacol.* **71**, 301–335 (2014).
79. R. J. Boado, Q. H. Zhou, J. Z. Lu, E. K. Hui, W. M. Pardridge, Pharmacokinetics and brain uptake of a genetically engineered bifunctional fusion antibody targeting the mouse transferrin receptor. *Mol. Pharm.* **7**, 237–244 (2010).
80. L. A. Horn *et al*., CD3xPDL1 bi-specific T cell engager (BiTE) simultaneously activates T cells and NKT cells, kills $PDL1^+$ tumor cells, and extends the survival of tumor-bearing humanized mice. *Oncotarget* **8**, 57964–57980 (2017).
81. C. P. Day, G. Merlino, T. Van Dyke, Preclinical mouse cancer models: A maze of opportunities and challenges. *Cell* **163**, 39–53 (2015).